Dinger, M. E., Mercer, T. R., and Mattick, J. S. (2008). RNAs as extracellular signaling molecules. *J. Mol. Endocrinol.* 40, 151–159.

Dunoyer, P., Schott, G., Himber, C., Meyer, D., Takeda, A., Carrington, J. C., and Voinnet, O. (2010). Small RNA duplexes function as mobile silencing signals between plant cells. *Science* 328, 912–916.

Duxbury, M. S., Ashley, S. W., and Whang, E. E. (2005). RNA interference: a mammalian SID-1 homologue enhances siRNA uptake and gene silencing efficacy in human cells. *Biochem. Biophys. Res. Commun.* 3, 459–463.

Feinberg, E. H., and Hunter, C. P. (2003). Transport of dsRNA into cells by the transmembrane protein SID-1. *Science* 12, 1545–1547.

Fleischhacker, M., and Schmidt, B. (2007). Circulating nucleic acids (CNAs) and cancer – a survey. *Biochim. Biophys. Acta* 1775, 181–232.

Galand, P., and Ledoux, L. (1966). Uptake of exogenous ribonucleic acid by ascites tumor cells. II. Relations between RNA uptake and the cellular metabolism. *Exp. Cell Res.* 43, 391–397.

Garzon, R., Marcucci, G., and Croce, C. M. (2010). Targeting microRNAs in cancer: rationale, strategies and challenges. *Nat. Rev. Drug Discov.* 9, 775–789.

Gibbings, D. J., Ciaudo, C., Erhardt, M., and Voinnet, O. (2009). Multivesicular bodies associate with components of miRNA effector complexes and modulate miRNA activity. *Nat. Cell Biol.* 11, 1143–1149.

Gourzones, C., Gelin, A., Bombik, I., Klibi, J., Verillaud, B., Guigay, J., Lang, P., Temam, S., Schneider, V., Amiel, C., Baconnais, S., Jimenez, A. S., and Busson, P. (2010). Extracellular release and blood diffusion of BART viral micro-RNAs produced by EBV-infected nasopharyngeal carcinoma cells. *Virol. J.* 7, 271.

Hanahan, D., and Weinberg, R. A. (2011). Hallmarks of cancer: the next generation. *Cell* 144, 646–674.

Hood, J. L., San, R. S., and Wickline, S. A. (2011). Exosomes released by melanoma cells prepare sentinel lymph nodes for tumor metastasis. *Cancer Res.* 71, 3792–3801.

Jose, A. M., Smith, J. J., and Hunter, C. P. (2009). Export of RNA silencing from *C. elegans* tissues does not require the RNA channel SID-1. *Proc. Natl. Acad. Sci. U.S.A.* 106, 2283–2288.

Kogure, T., Lin, W. L., Yan, I. K., Braconi, C., and Patel, T. (2011). Intercellular nanovesicle-mediated microRNA transfer: a mechanism of environmental modulation of hepatocellular cancer cell growth. *Hepatology* 54, 1237–1248.

Kolodny, G. M. (1971). Evidence for transfer of macromolecular RNA between mammalian cells in culture. *Exp. Cell Res.* 65, 313–324.

Kosaka, N., Iguchi, H., and Ochiya, T. (2010a). Circulating microRNA in body fluid: a new potential biomarker for cancer diagnosis and prognosis. *Cancer Sci.* 101, 2087–2092.

Kosaka, N., Iguchi, H., Yoshioka, Y., Takeshita, F., Matsuki, Y., and Ochiya, T. (2010b). Secretory mechanisms and intercellular transfer of microRNAs in living cells. *J. Biol. Chem.* 285, 17442–17452.

Kuwabara, Y., Ono, K., Horie, T., Nishi, H., Nagao, K., Kinoshita, M., Watanabe, S., Baba, O., Kojima, Y., Shizuta, S., Imai, M., Tamura, T., Kita, T., and Kimura, T. (2011). Increased microRNA-1 and microRNA-133a levels in serum of patients with cardiovascular disease indicate the existence of myocardial damage. *Circ. Cardiovasc. Genet.* 4, 446–454.

Kwak, P. B., Iwasaki, S., and Tomari, Y. (2011). The microRNA pathway and cancer. *Cancer Sci.* 101, 2309–2315.

Lawrie, C. H., Gal, S., Dunlop, H. M., Pushkaran, B., Liggins, A. P., Pulford, K., Banham, A. H., Pezzella, F., Boultwood, J., Wainscoat, J. S., Hatton, C. S., and Harris, A. L. (2008). Detection of elevated levels of tumour-associated microRNAs in serum of patients with diffuse large B-cell lymphoma. *Br. J. Haematol.* 141, 672–675.

Lim, P. K., Bliss, S. A., Patel, S. A., Taborga, M., Dave, M. A., Gregory, L. A., Greco, S. J., Bryan, M., Patel, P. S., and Rameshwar, P. (2011). Gap junction-mediated import of microRNA from bone marrow stromal cells can elicit cell cycle quiescence in breast cancer cells. *Cancer Res.* 71, 1550–1560.

Mandel, P., and Metais, P. (1947). Les acides nucleiques du plasma sanguin chez l'homme. *C. R. Acad. Sci. Paris* 142, 241–243.

Mittelbrunn, M., Gutierrez-Vazquez, C., Villarroya-Beltri, C., Gonzalez, S., Sanchez-Cabo, F., Gonzalez, M. A., Bernad, A., and Sanchez-Madrid, F. (2011). Unidirectional transfer of microRNA-loaded exosomes from T cells to antigen-presenting cells. *Nat. Commun.* 2, 282.

Molnar, A., Melnyk, C. W., Bassett, A., Hardcastle, T. J., Dunn, R., and Baulcombe, D. C. (2010). Small silencing RNAs in plants are mobile and direct epigenetic modification in recipient cells. *Science* 328, 872–875.

Muralidharan-Chari, V., Clancy, J. W., Sedgwick, A., and D'Souza-Schorey, C. (2010). Microvesicles: mediators of extracellular communication during cancer progression. *J. Cell. Sci.* 15, 1603–1611.

Pegtel, D. M., Cosmopoulos, K., Thorley-Lawson, D. A., Van Eijndhoven, M. A., Hopmans, E. S., Lindenberg, J. L., De Gruijl, T. D., Wurdinger, T., and Middeldorp, J. M. (2010). Functional delivery of viral miRNAs via exosomes. *Proc. Natl. Acad. Sci. U.S.A.* 107, 6328–6333.

Reddi, K. K., and Holland, J. F. (1976). Elevated serum ribonuclease in patients with pancreatic cancer. *Proc. Natl. Acad. Sci. U.S.A.* 73, 2308–2310.

Rieber, M., and Bacalao, J. (1974). An "external" RNA removable from mammalian cells by mild proteolysis. *Proc. Natl. Acad. Sci. U.S.A.* 71, 4960–4964.

Stroun, M., Anker, P., Beljanski, M., Henri, J., Lederrey, C., Ojha, M., and Maurice, P. A. (1978). Presence of RNA in the nucleoprotein complex spontaneously released by human lymphocytes and frog auricles in culture. *Cancer Res.* 38, 3546–3554.

Trajkovic, K., Hsu, C., Chiantia, S., Rajendran, L., Wenzel, D., Wieland, F., Schwille, P., Brugger, B., and Simons, M. (2008). Ceramide triggers budding of exosome vesicles into multivesicular endosomes. *Science* 319, 1244–1247.

Tsui, N. B., Ng, E. K., and Lo, Y. M. (2002). Stability of endogenous and added RNA in blood specimens, serum, and plasma. *Clin. Chem.* 48, 1647–1653.

Turchinovich, A., Weiz, L., Langheinz, A., and Burwinkel, B. (2011). Characterization of extracellular circulating microRNA. *Nucleic Acids Res.* 39, 7223–7233.

Valadi, H., Ekstrom, K., Bossios, A., Sjostrand, M., Lee, J. J., and Lotvall, J. O. (2007). Exosome-mediated transfer of mRNAs and microRNAs is a novel mechanism of genetic exchange between cells. *Nat. Cell Biol.* 9, 654–659.

Vickers, K. C., Palmisano, B. T., Shoucri, B. M., Shamburek, R. D., and Remaley, A. T. (2011). MicroRNAs are transported in plasma and delivered to recipient cells by high-density lipoproteins. *Nat. Cell Biol.* 13, 423–433.

Wang, K., Zhang, S., Weber, J., Baxter, D., and Galas, D. J. (2010). Export of microRNAs and microRNA-protective protein by mammalian cells. *Nucleic Acids Res.* 38, 7248–7259.

Watson, J. D., and Crick, F. H. (1953). Molecular structure of nucleic acids; a structure for deoxyribose nucleic acid. *Nature* 171, 737–738.

Wieczorek, A. J., Sitaramam, V., Machleidt, W., Rhyner, K., Perruchoud, A. P., and Block, L. H. (1987). Diagnostic and prognostic value of RNA-proteolipid in sera of patients with malignant disorders following therapy: first clinical evaluation of a novel tumor marker. *Cancer Res.* 47, 6407–6412.

Zernecke, A., Bidzhekov, K., Noels, H., Shagdarsuren, E., Gan, L., Denecke, B., Hristov, M., Koppel, T., Jahantigh, M. N., Lutgens, E., Wang, S., Olson, E. N., Schober, A., and Weber, C. (2009). Delivery of microRNA-126 by apoptotic bodies induces CXCL12-dependent vascular protection. *Sci. Signal.* 2, ra81.

Zhang, L., Hou, D., Chen, X., Li, D., Zhu, L., Zhang, Y., Li, J., Bian, Z., Liang, X., Cai, X., Yin, Y., Wang, C., Zhang, T., Zhu, D., Zhang, D., Xu, J., Chen, Q., Ba, Y., Liu, J., Wang, Q., Chen, J., Wang, J., Wang, M., Zhang, Q., Zhang, J., Zen, K., and Zhang, C. Y. (2011). Exogenous plant MIR168a specifically targets mammalian LDLRAP1: evidence of cross-kingdom regulation by microRNA. *Cell Res.* PMID: 21931358. [Epub ahead of print].

Zhang, Y., Liu, D., Chen, X., Li, J., Li, L., Bian, Z., Sun, F., Lu, J., Yin, Y., Cai, X., Sun, Q., Wang, K., Ba, Y., Wang, Q., Wang, D., Yang, J., Liu, P., Xu, T., Yan, Q., Zhang, J., Zen, K., and Zhang, C. Y. (2010). Secreted monocytic miR-150 enhances targeted endothelial cell migration. *Mol. Cell* 39, 133–144.

Conflict of Interest Statement: The authors declare that the research was conducted in the absence of any commercial or financial relationships that could be construed as a potential conflict of interest.

Received: 29 August 2011; paper pending published: 20 September 2011; accepted: 08 December 2011; published online: 03 January 2012.

Citation: Kosaka N and Ochiya T (2012) Unraveling the mystery of cancer by secretory microRNA: horizontal microRNA transfer between living cells. Front. Gene. 2:97. doi: 10.3389/fgene.2011.00097

This article was submitted to Frontiers in Non-Coding RNA, a specialty of Frontiers in Genetics.

Int. J. Mol. Sci. **2012**, *13*, 8259-8272; doi:10.3390/ijms13078259

OPEN ACCESS
International Journal of
Molecular Sciences
ISSN 1422-0067
www.mdpi.com/journal/ijms

Article

Genome-Wide Analysis of DNA Methylation and Expression of MicroRNAs in Breast Cancer Cells

Sumiyo Morita [1], Ryou-u Takahashi [2], Riu Yamashita [3], Atsushi Toyoda [4], Takuro Horii [1], Mika Kimura [1], Asao Fujiyama [4], Kenta Nakai [5], Shoji Tajima [6], Ryo Matoba [7], Takahiro Ochiya [2] and Izuho Hatada [1,*]

1 Laboratory of Genome Science, Biosignal Genome Resource Center, Institute for Molecular and Cellular Regulation, Gunma University, Gunma 371-8512, Japan; E-Mails: msumiyo@gunma-u.ac.jp (S.M.); horii@gunma-u.ac.jp (T.H.); mikimura@showa.gunma-u.ac.jp (M.K.)

2 Division of Molecular and Cellular Medicine, National Cancer Center Research Institute, 5-1-1, Tsukiji, Chuo-ku, Tokyo 104-0045, Japan; E-Mails: rytakaha@ncc.go.jp (R.T.); tochiya@ncc.go.jp (T.O.)

3 Department of Integrative Genomics, Medical Megabank Organization, Tohoku University, 6-3-09, aza Aoba, Aramaki, Aobaku, Sendai 980-8579, Japan; E-Mail: ryamasi@megabank.tohoku.ac.jp

4 Center for Genetic Resource Information, National Institute of Genetics, Shizuoka 411-8540, Japan; E-Mails: atoyoda@lab.nig.ac.jp (A.T.); afujiyam@lab.nig.ac.jp (A.F.)

5 Human Genome Center, Institute of Medical Science, University of Tokyo, 4-6-1 Shirokanedai, Minato-ku, Tokyo 108-8639, Japan; E-Mail: knakai@ims.u-tokyo.ac.jp

6 Laboratory of Epigenetics, Institute for Protein Research, Osaka University, 3-2 Yamadaoka, Suita, Osaka 565-0871, Japan; E-Mail: tajima@protein.osaka-u.ac.jp

7 DNA Chip Research Inc., 1-1-43 Suehirocho, Tsurumi-ku, Yokohama, Kanagawa 230-0045, Japan; E-Mail: matoba@dna-chip.co.jp

* Author to whom correspondence should be addressed; E-Mail: hatada@gunma-u.ac.jp; Tel.: +81-27-220-8057; Fax: +81-27-220-8110.

Received: 30 May 2012; in revised form: 19 June 2012 / Accepted: 27 June 2012 / Published: 3 July 2012

Abstract: DNA methylation of promoters is linked to transcriptional silencing of protein-coding genes, and its alteration plays important roles in cancer formation. For example, hypermethylation of tumor suppressor genes has been seen in some cancers. Alteration of methylation in the promoters of microRNAs (miRNAs) has also been linked to transcriptional changes in cancers; however, no systematic studies of methylation and

transcription of miRNAs have been reported. In the present study, to clarify the relation between DNA methylation and transcription of miRNAs, next-generation sequencing and microarrays were used to analyze the methylation and expression of miRNAs, protein-coding genes, other non-coding RNAs (ncRNAs), and pseudogenes in the human breast cancer cell lines MCF7 and the adriamycin (ADR) resistant cell line MCF7/ADR. DNA methylation in the proximal promoter of miRNAs is tightly linked to transcriptional silencing, as it is with protein-coding genes. In protein-coding genes, highly expressed genes have CpG-rich proximal promoters whereas weakly expressed genes do not. This is only rarely observed in other gene categories, including miRNAs. The present study highlights the epigenetic similarities and differences between miRNA and protein-coding genes.

Keywords: DNA methylation; microRNA; cancer

1. Introduction

DNA methylation plays important roles in development, differentiation, X inactivation, genomic imprinting, and silencing of transposable elements through the regulation of transcription [1–3]. This usually occurs in mammalian cells at cytosine residues in the context of cytosine-phosphate-guanine dinucleotide (CpG), and approximately 60%–90% of cytosines at these sites are methylated [4]. Methyl-CpG serves as the physiological ligand for a family of proteins containing a highly conserved methyl-CpG binding domain (MBD) [5]. These proteins recruit various chromatin-modifying complexes to methyl-CpG sites to cause further chromatin structural changes that result in transcriptional silencing.

Alterations of the patterns of normal DNA methylation result in many human diseases, including cancer [6]. Aberrant patterns of DNA methylation in cancers are associated with tumor type, stage, prognosis, and response to chemotherapy. Human tumors undergo global DNA demethylation, including of Line-1 repetitive elements, and then DNA hypermethylation of certain gene promoters, including those of tumor suppressor genes [7]. Aberrant DNA methylation in cancers is not restricted to protein-coding genes; it is also observed in microRNA (miRNA) genes. MicroRNAs are small noncoding regulatory RNAs of 20–24 nucleotides that reduce the stability and/or translation of fully or partially sequence-complementary target mRNAs. MicroRNAs can act as oncogenes or tumor suppressors, and can contribute to cancer initiation and progression [8].

Genome-wide analysis of DNA methylation is an important issue in epigenetic research. The oldest technology for genome-wide analysis of DNA methylation, Restriction Landmark Genomic Scanning, which utilizes two-dimensional gel electrophoresis of genomic DNA, was developed in 1991 [9,10]. This technology has been used in the cloning of many imprinted genes [10] and tumor suppressors [11,12]. In this century, development of genome-wide analysis technology such as microarrays and next-generation sequencers brought about several new methods for analyzing DNA methylation [13]. Among these methods, capture and next-generation sequencing of methyl-CpG

binding domains of MBD1 protein is especially useful for analysis because the binding activity of this protein is stronger than that of antibodies [14].

Although epigenetic silencing of miRNAs has been reported in many cancers, systematic studies of DNA methylation and miRNA transcription have not yet been reported. In addition, differentially methylated regions were found only in the CpG islands just upstream of miRNAs in most reports on the epigenetic silencing of miRNAs because such cases are easily discovered. Therefore, it has not been clarified whether the transcriptional start sites far upstream of miRNAs are influenced by DNA methylation or not. It has also not been clarified whether the CpG-poor promoters of miRNA are influenced by DNA methylation. Furthermore, miRNAs are not only transcribed by RNA polymerase II, which is responsible for most protein-coding genes, but also transcribed by RNA polymerase III. Although the relation between DNA methylation and silencing has been extensively studied in genes transcribed by RNA polymerase II, there are few reports for genes transcribed by RNA polymerase III. Therefore, systematic analyses of the methylation and expression of miRNAs are required. To clarify the relation between DNA methylation and transcription of miRNAs, here we systematically analyzed the methylation and expression of human genes encoding miRNAs, proteins, other non-coding RNAs (ncRNAs), and pseudogenes using next-generation sequencing and microarray analysis.

2. Results and Discussion

2.1. Genome-Wide Identification of Methylated DNA

To study the genome-wide methylation signature, we performed massive sequencing of methylated DNA enriched by the MBD domain of MBD1, using an Illumina sequencer. We expressed a His-tagged fragment of MBD1 (aa 1–75) in bacteria. This fragment contains the critical MBD domain required for stable and selective binding to methyl-CpG but no structural elements known to contribute to sequence-specific DNA binding [15]. Randomly shared methylated genomic DNA (about 300 bp) was bound to His- and GST-tagged fragments of MBD1 and collected on Dynabeads Talon Magnetic beads, which bind to the His tag. The collected DNA was then purified and sequenced using a next-generation sequencer (Illumina). We performed the genome-wide methylation analysis on a human breast cancer-derived cell line, MCF7, and an adriamycin resistant cancer cell line MCF7/ADR [16]. We obtained 19 million single-end reads for MCF7 and MCF7/ADR with high quality read placement against the human genome.

To determine the reliability of our genome-wide analysis of DNA methylation, the methylation signature attained in our analysis was confirmed using previous reports. Several genes were reported to be differentially methylated between MCF7 and MCF7/ADR. For example, ABCB1 (MDR1), encoding P-glycoprotein, which is capable of mediating resistance to many antineoplastic drugs commonly used to treat breast cancer by acting as an efflux pump, is hypermethylated in MCF7 but demethylated and overexpressed in drug-resistant MCF7/ADR [17]. We confirmed this differential methylation between MCF7 and MCF7/ADR in our analyzed data (Figure 1a). The silencing of CDH1, which encodes E-cadherin, is important in the epithelial-to-mesenchymal transition. It has been reported by others [18] and confirmed by our results that CDH1 is unmethylated in MCF7 but

hypermethylated in MCF7/ADR (Figure 1b). Differential methylation of TGM2 [19], a potential molecular marker for chemotherapeutic drug sensitivity, was also confirmed (Figure 1c).

Figure 1. Representative methyl-CpG binding domain (MBD)1DIP-Seq profiles of previously reported differentially methylated promoters between MCF7 and MCF7/adriamycin (ADR). *Y* axis represents the methylation levels of each cell line. Arrows and green bars denote transcription start sites and cytosine-phosphate-guanine dinucleotide (CpG) islands, respectively. (**a**) P-glycoprotein (ABCB1) locus; (**b**) E-cadherin (CDH1) locus; (**c**) transglutaminase 2 gene (TGM2) locus.

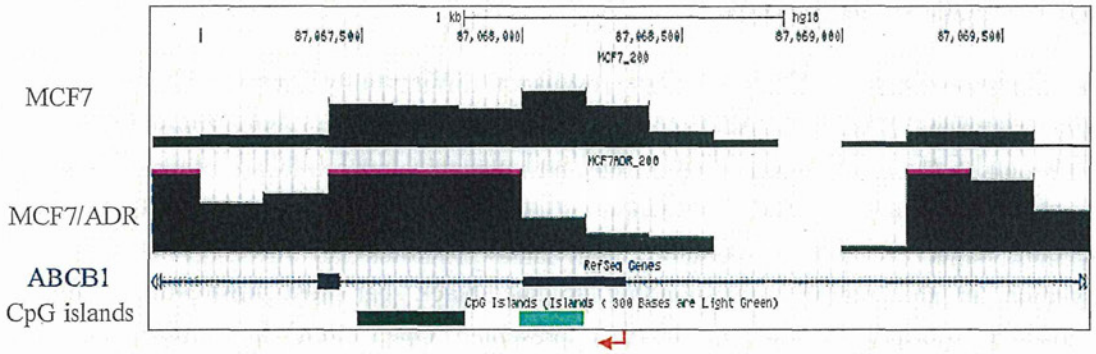

(a)

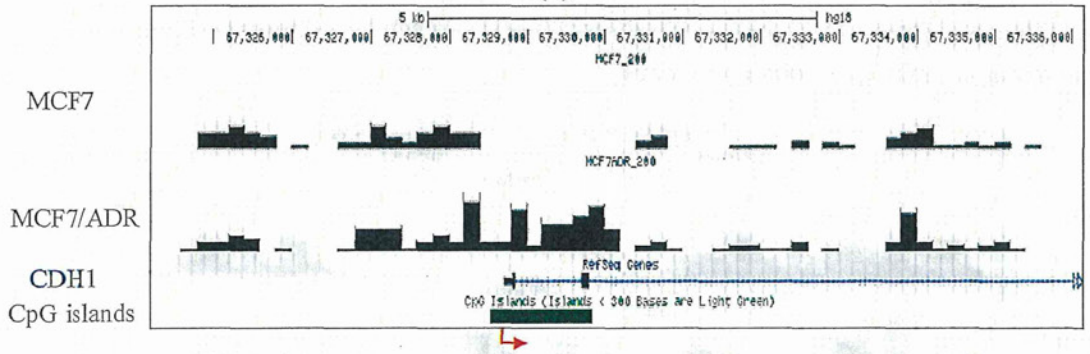

(b)

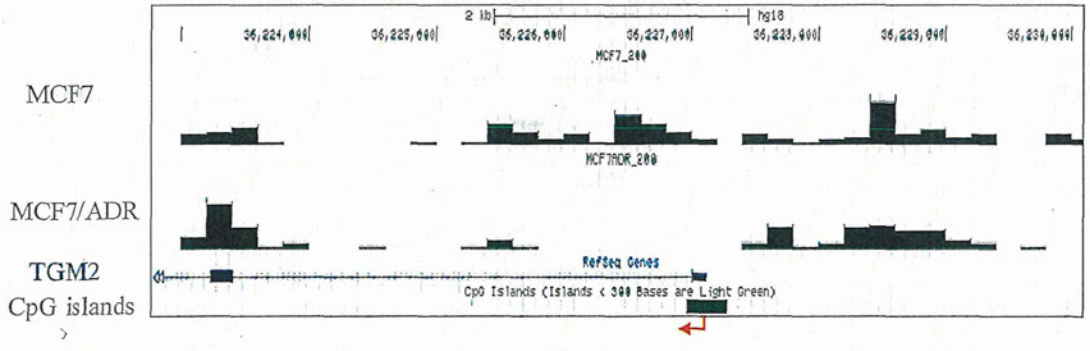

(c)

Next, we compared the methylation around the miRNA promoters between MCF7 and MCF7/ADR and pick up the differentially methylated regions. By confirming these differentially methylated regions using bisulfite sequencing, we tested the reliability of our analysis. Combining nucleosome mapping with chromatin signatures of promoters, 157 proximal promoters of human miRNA [20] were

identified and used for the analysis. We found several miRNA clusters, such as miR-200c/141 and miR-200ab/429, which were differentially methylated between these cell lines. For example, the proximal promoter of the miR-200c/141 cluster was hypermethylated in drug-resistant MCF7/ADR (Figure 2a), a finding confirmed by bisulfite sequencing (Figure 2b). In addition, the expression of these miRNAs was downregulated in MCF7/ADR (Figure 2c). Silencing of miR-200 families is important for the maintenance of breast cancer stem cells [21]. This family is also important for the regulation of the epithelial to mesenchymal transition [22] and drug-resistance [23]. The proximal promoter of the miR-200ab/429 cluster was also hypermethylated in MCF7/ADR (Figure 2d), and this was also confirmed to be silenced (data not shown). These results confirmed the reliability of our MBD1-based DNA methylation analysis.

Figure 2. Representative MBD1DIP-Seq profiles of differentially methylated miRNA promoters between MCF7 and MCF7/ADR. Arrows and green bars denote transcription start sites and CpG islands, respectively. Red and magenta blocks indicate pre-miRNAs and scaRNAs, respectively. (**a**) Methylation of the miR-200c/141 locus; (**b**) Bisulfite sequencing results for the differentially methylated promoter of miR-200c/141. The methylation in the region corresponding to the black bar just upstream of the miR-200c/141 transcription start site in (**a**) is presented. Open circles and closed circles denote unmethylated and methylated CpG sites, respectively; (**c**) Real-time-PCR analysis of miR-200c and miR-141 expression. Expression level in MCF7 is normalized as 100%; (**d**) Methylation of the mir-200ab/429 locus.

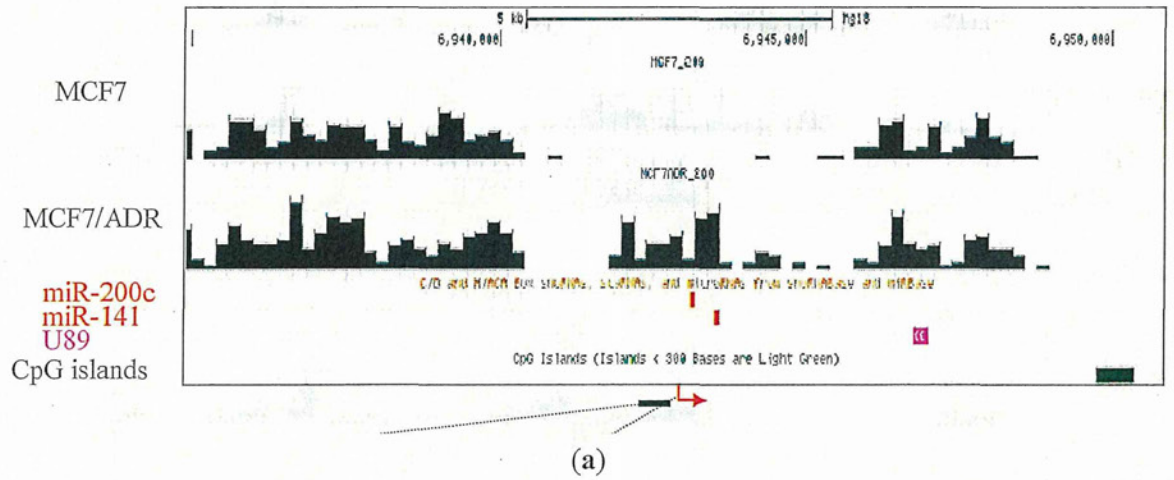

(a)

Figure 2. *Cont.*

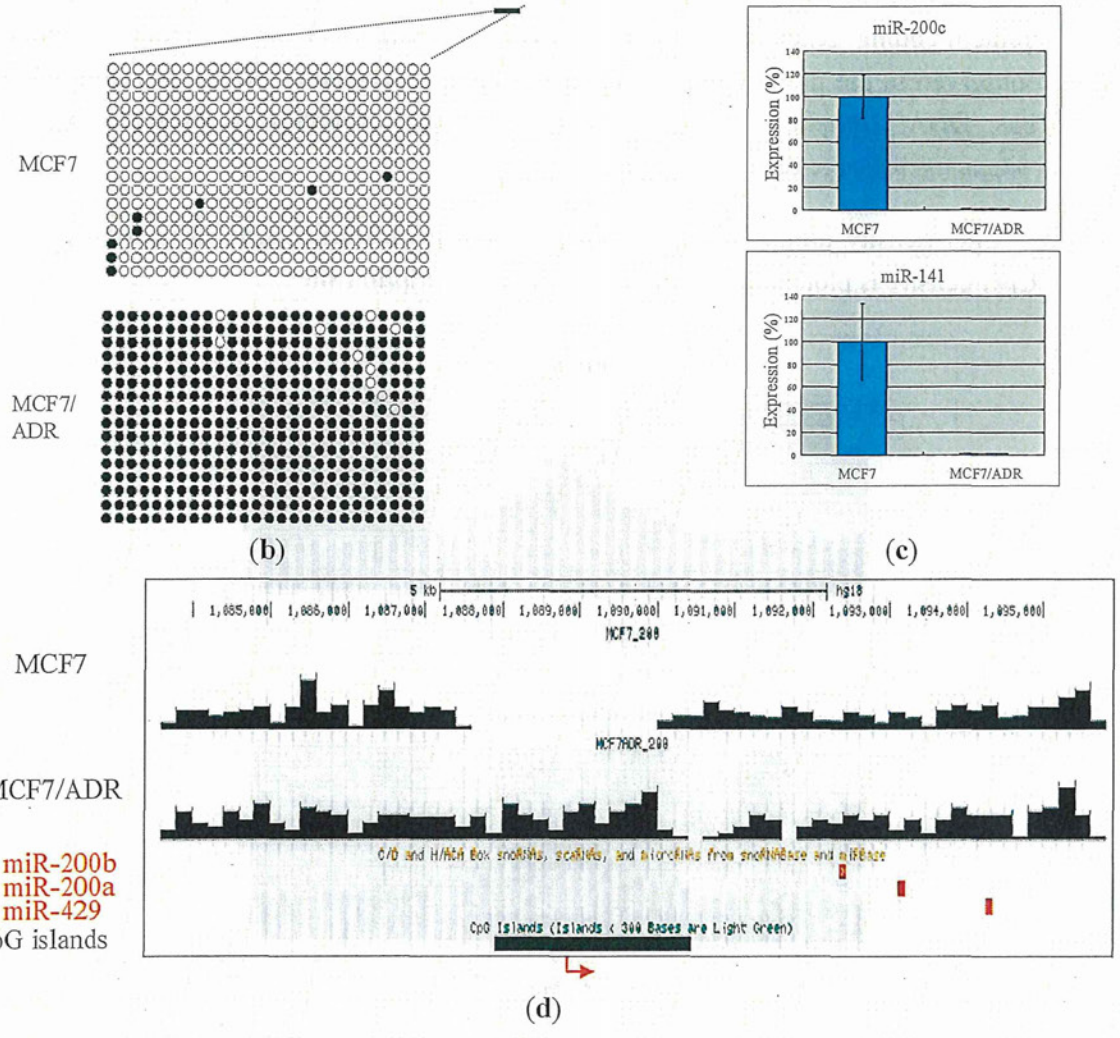

2.2. DNA Methylation versus *Transcription*

To explore the relationship between gene expression and DNA methylation in the proximal promoter and elsewhere in the gene, we performed microarray analysis using the Agilent platform for miRNA and ordinary genes in MCF7. We were able to use 157 miRNAs, 600 RefSeq non-coding RNAs (ncRNAs) and 235 RefSeq pseudogenes for both expression and methylation analysis. We also used 1000 randomly selected RefSeq protein-coding genes. Before analysis, we plotted the CpG density of each gene category against the position in the genes, since CpG density is an important promoter characteristic. For genes of all categories, the highest CpG density was at the transcription start site, and this is characteristic of promoters (Figure 3). miRNA and protein-coding genes had higher CpG density at the transcription start site compared with other non-coding RNA genes and pseudogenes (Figure 3). We split the genes into two groups: "highly expressed" and "weakly expressed" genes. Highly expressed and weakly expressed genes were defined as those falling within the highest 20% expression quantile and the lowest 20% expression quantile, respectively. For each group, we plotted average cytosine methylation against gene position (Figure 4). This analysis was

performed for each category of gene: miRNA, protein-coding, other non-coding RNA, and pseudogene. In the highly expressed genes, we observed low methylation in the proximal promoters for both miRNAs and protein-coding genes (Figure 4). However, low methylation in the highly expressed genes was not observed in the proximal promoters for the other non-coding RNAs and pseudogenes (Figure 4). Thus, DNA methylation in the proximal promoter of miRNAs is tightly linked to transcriptional silencing, as is the case with protein-coding genes.

Figure 3. CpG density around the transcription start site for each gene category. The average CpG density is plotted against distance from transcription site.

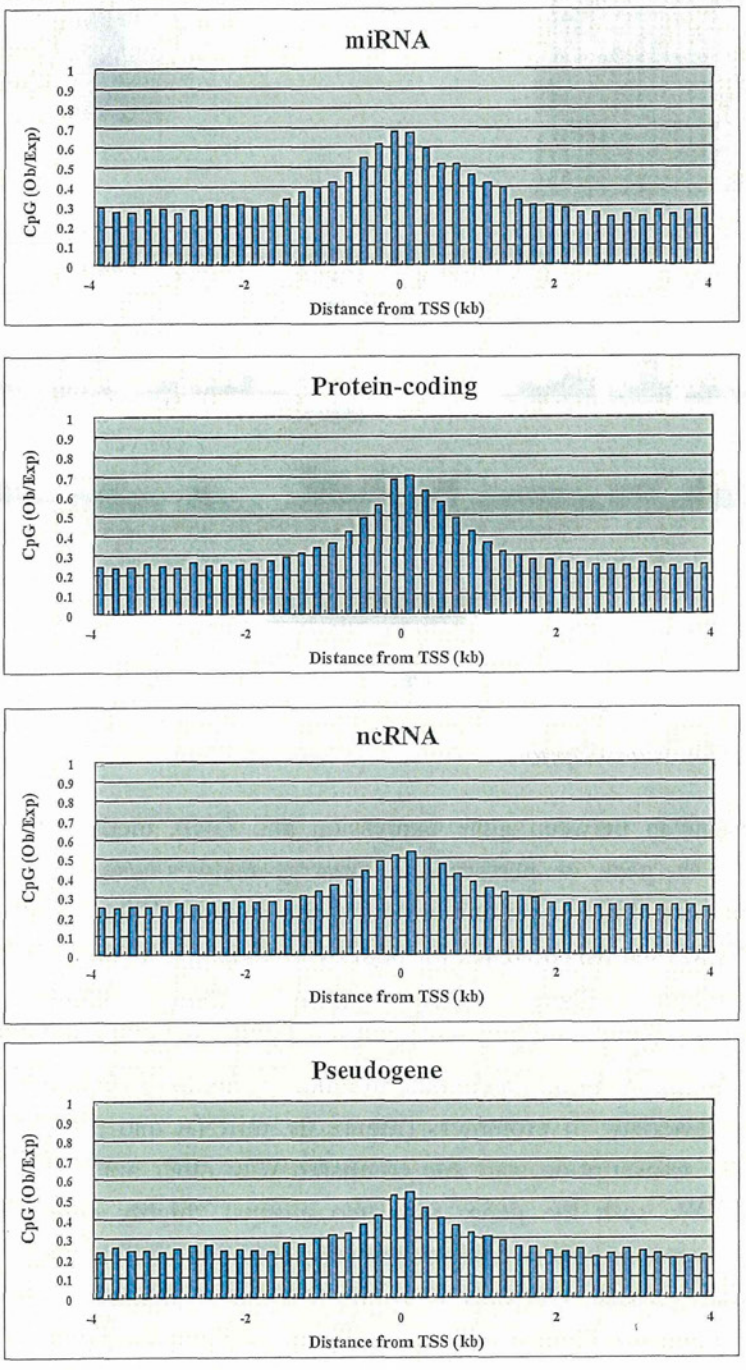

Figure 4. Methylation of weakly expressed and highly expressed genes. The average methylation for each gene category is plotted against distance from transcription start site.

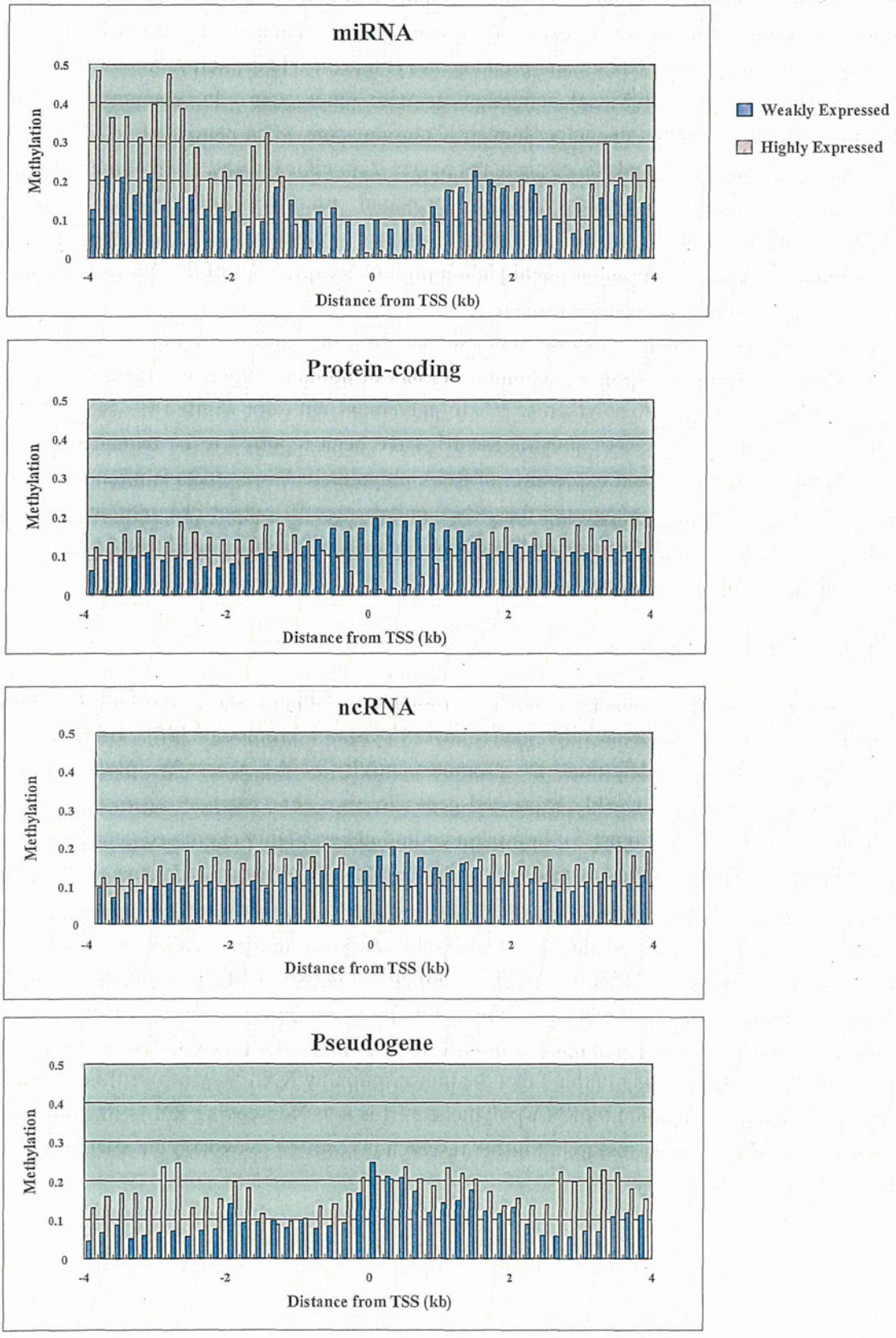

In addition to proximal promoter methylation, the role of non-promoter methylation, such as in enhancers/far-upstream elements and within the body of the gene, was also examined. Methylation was seen in the gene body and far upstream region, with highly expressed genes showing more extensive methylation compared with weakly expressed genes in all categories, including miRNAs, protein-coding, other non-coding RNAs, and pseudogenes (Figure 4). Thus, non-promoter methylation of miRNAs is linked to transcriptional activation, as with other genes. In mammals, gene-body methylation has been observed in the active human X chromosome when compared with its inactive counterpart [24]. Genome-wide analysis of postnatal neural stem cells indicates that Dnmt3a occupies and methylates non-promoter regions flanking proximal promoters of a large cohort of transcriptionally active genes, many of which encode regulators of neurogenesis [25]. Dnmt3a-dependent nonproximal promoter methylation promotes expression of these neurogenic genes by functionally antagonizing Polycomb repression.

Thus, our genome-wide analysis demonstrated for the first time that the relation between DNA methylation and transcription of miRNAs are similar to that of protein-coding genes although some of miRNAs are transcribed by RNA polymerase III. In agreement with our results, U6 snRNA family genes, which are transcribed by RNA polymerase III, have been reported to be regulated by DNA methylation recently [26]. Increased expression of RNA polymerase III products is often observed in transformed cells [27]. It is also suggested that RNA polymerase III output can substantially affect transformation [27]. Therefore, transcriptional regulation of miRNAs transcribed by RNA polymerase III might play an important role in transformation.

2.3. *CpG Density* versus *Transcription*

CpG density underlies many characteristics of promoters. Ubiquitously expressed genes have CpG-rich promoters, while tissue-specific genes have CpG-poor promoters [28]. Therefore, it is possible that CpG density can determine the promoter activity of the genes. We plotted the CpG density of highly expressed and weakly expressed genes in each gene category against the position from the transcription start site (Figure 5). In protein-coding genes, highly expressed genes had higher CpG density in the promoter, while weakly expressed genes had lower CpG density (Figure 5). In other words, ubiquitously expressed genes have stronger promoter activity compared with tissue-specific genes. This characteristic is only weakly observed in gene categories other than protein-coding genes (Figure 5). Therefore, this correlation between CpG density and promoter activity could be related to protein-coding ability. Protein-coding genes are transcribed by RNA polymerase II, while genes coding small non-coding RNAs including some miRNAs are transcribed by RNA polymerase III. It is intriguing to think that the transcription by RNA polymerase II is affected by CpG density, while the transcription by RNA polymerase III is not. Non-coding RNAs including small RNA become important in cancer research. Further research is required to explain the relation between CpG density and promoter activity.

Figure 5. CpG density of weakly expressed and highly expressed genes. The average CpG density of each gene category is plotted against distance from transcription site.

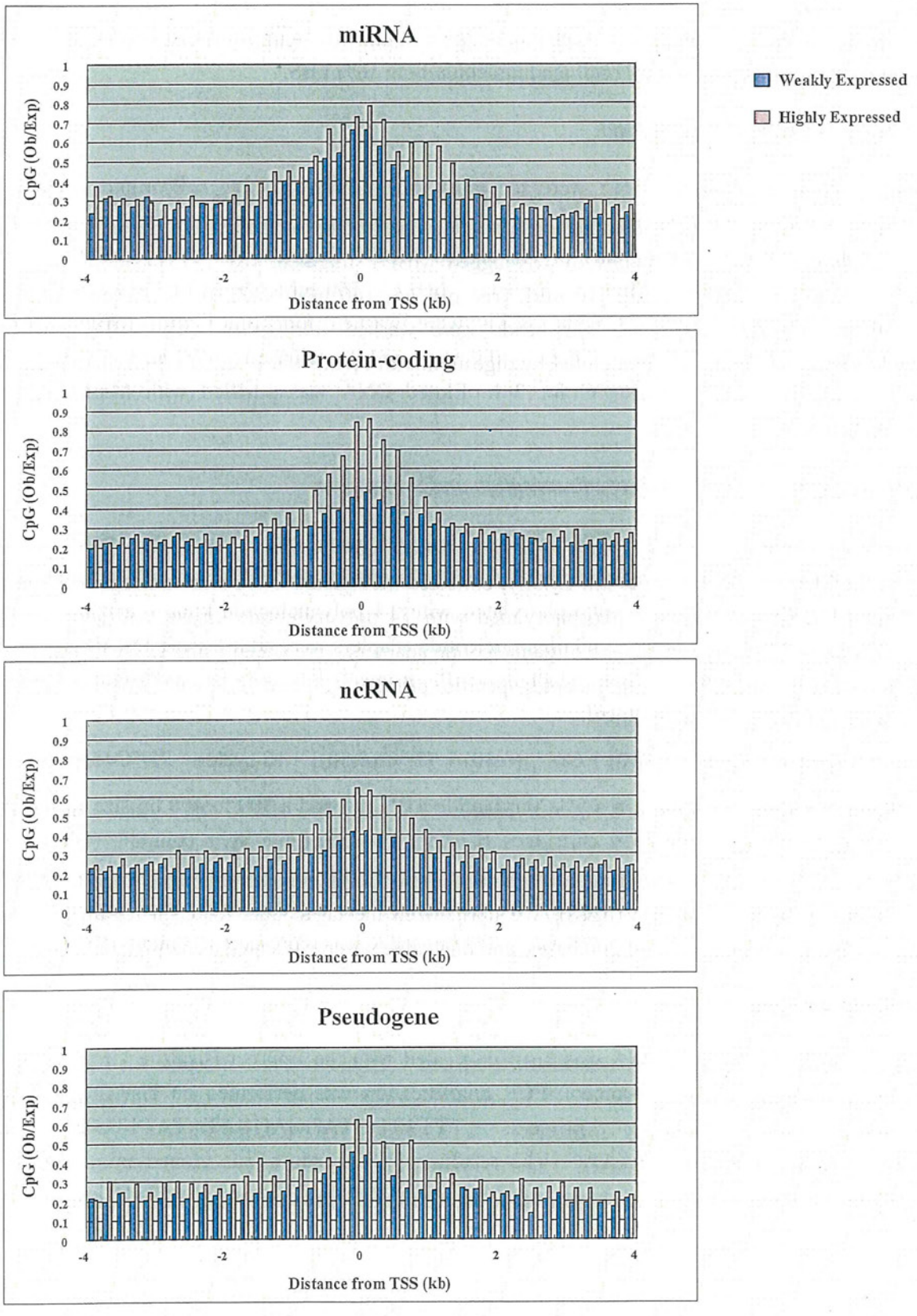

3. Experimental Section

3.1. Cell Lines and Culture Conditions

The human breast cancer-derived cell line, MCF7, and its multi-drug resistant derivative, MCF7/ADR, were cultured in RPMI1640 medium containing 10% FBS.*

3.2. Isolation of Methyl-DNA by MBD1

Ten micrograms of genomic DNA were sonicated to 100–500 bp using a Bioruptor UCD-250 (Cosmo Bio, Tokyo) sonicator. The capture reaction was performed by adding 10 mg of sonicated DNA to a mixture of 10 micrograms of His-tagged MBD1 fragment (aa 1–75) and 60 μL of Dynabeads TALON in MBD1 buffer (10 mM Tris, pH 7.5, 160 mM NaCl, 0.1% Tween20) on a rotating mixer, overnight, at 4 °C. The beads were washed four times with MBD1 buffer. The bound methylated DNA was then eluted by digestion with Proteinase K in 50 mM Tris (pH 7.5), 10 mM EDTA, 0.5% SDS, at 50 °C for 3 h. Eluted DNA was purified with MinElute spin columns (QIAGEN).

3.3. Illumina Genome Analyzer Library Preparation and Sequencing

A single-end library was made following the modified manufacturer's protocol with reagents supplied in the Illumina DNA sample kit. Briefly, collected methylated DNA was end-repaired using Klenow and T4 DNA polymerases, phosphorylated with T4 polynucleotide kinase, and adenylated using Klenow exo-DNA polymerase, and oligonucleotide adapters were added using DNA ligase. The ligated product was amplified using adapter-specific primers 1.1 and 2.1 with Phusion DNA polymerase using the following protocol:

$$98\ ^\circ C\ (0{:}30) + [98\ ^\circ C\ (0{:}10) + 65\ ^\circ C\ (0{:}30) + 72\ ^\circ C\ (0{:}30)] \times 10\ \text{cycles} + 72\ ^\circ C\ (5{:}00)$$

Amplified DNA was visualized in a 5% Acrylamide TBE gel, and a 300 to 400 bp size range was excised and purified using SPIN-X cartridges (Costar) and MinElute spin columns (QIAGEN). A single-flow cell lane was sequenced in an Illumina Genome Analyzer. The reds were mapped to the reference human genome sequences (hg18). We normalized the tag counts for each region to tags per million (ppm) in a window size of 200 bases, and this value was represented as methylation level.

3.4. Bisulfite Sequencing

One microgram of genomic DNA was bisulfite-treated with the EpiTect Bisulfite kit (QIAGEN) according to the manufacturer's protocol. PCR amplification was performed on bisulfite-modified DNA using the following primers: TTTATGGTAGGAGGATATATTTGTG and CACCTTAAATCAAACAACTTCAAAC. The resulting PCR product was cloned into a pCR2.1 (Invitrogen) TA-cloning vector and was sequenced using a 3130 DNA sequencer (Applied Biosystems).

3.5. Real-Time PCR Analysis of miRNA Expression

Expression of mature miRNAs (miR-200c and miR-141) in human breast cancer cell lines was analyzed by TaqMan miRNA Assay (Applied Biosystems) under conditions defined by the supplier.

3.6. Genome-Wide Gene Expression Analysis

Expression analysis of miRNA and the other genes was carried out using Agilent's microarray-based miRNA and mRNA platforms, respectively. Labeling and hybridization was performed according to the manufacturer's protocol (Agilent Technologies).

4. Conclusions

In this study, we systematically analyzed the methylation and expression of human miRNAs in breast cancer cell lines and compared these levels with those of other gene categories using next-generation sequencing and microarray analysis. We found that DNA methylation in the proximal promoters of miRNAs and protein-coding genes was tightly linked to transcriptional silencing. Expression analysis revealed a correlation between expression level and CpG density of proximal promoters in protein-coding genes; however, this was only weakly observed in miRNA genes. Our observations highlight the epigenetic similarities and differences between miRNA and protein-coding genes.

Acknowledgments

This work was supported in part by grants from the Ministry of Education, Culture, Sports, Science and Technology of Japan; the Ministry of Health, Labour and Welfare of Japan; the National Institute of Biomedical Innovation; and the Takeda Science Foundation.

References

1. Ohgane, J.; Aikawa, J.; Ogura, A.; Hattori, N.; Ogawa, T.; Shiota, K. Analysis of CpG islands of trophoblast giant cells by restriction landmark genomic scanning. *Dev. Genet.* **1998**, *22*, 132–140.
2. Song, F.; Smith, J.F.; Kimura, M.T.; Morrow, A.D.; Matsuyama, T.; Nagase, H.; Held, W.A. Association of tissue-specific differentially methylated regions (TDMs) with differential gene expression. *Proc. Natl. Acad. Sci. USA* **2005**, *102*, 3336–3341.
3. Klose, R.J.; Bird, A.P. Genomic DNA methylation: The mark and its mediators. *Trends Biochem. Sci.* **2006**, *31*, 89–97.
4. Razin, A.; Webb, C.; Szyf, M.; Yisraeli, J.; Rosenthal, A.; Naveh-Many, T.; Sciaky-Gallili, N.; Cedar, H. Variations in DNA methylation during mouse cell differentiation *in vivo* and *in vitro*. *Proc. Natl. Acad. Sci.USA* **1984**, *81*, 2275–2279.
5. Bird, A.P.; Wolffe, A.P. Methylation-induced repression—Belts, braces, and chromatin. *Cell* **1999**, *99*, 451–454.
6. Feinberg, A.P.; Tycko, B. The history of cancer epigenetics. *Nat. Rev. Cancer* **2004**, *4*, 143–153.

7. Herman, J.G.; Baylin, S.B. Gene silencing in cancer in association with promoter hypermethylation. *N. Engl. J. Med.* **2003**, *349*, 2042–2054.
8. Zhang, B.; Pan, X.; Cobb, G.P.; Anderson, T.A. microRNAs as oncogenes and tumor suppressors. *Dev. Biol.* **2007**, *302*, 1–12.
9. Hatada, I.; Hayashizaki, Y.; Hirotsune, S.; Komatsubara, H.; Mukai, T. A genomic scanning method for higher organisms using restriction sites as landmarks. *Proc. Natl. Acad. Sci. USA* **1991**, *88*, 9523–9527.
10. Hatada, I.; Sugama, T.; Mukai, T. A new imprinted gene cloned by a methylation-sensitive genome scanning method. *Nucleic. Acids. Res.* **1993**, *21*, 5577–5582.
11. Yoshikawa, H.; Matsubara, K.; Qian, G.S.; Jackson, P.; Groopman, J.D.; Manning, J.E.; Harris, C.C.; Herman, J.G. SOCS-1, a negative regulator of the JAK/STAT pathway, is silenced by methylation in human hepatocellular carcinoma and shows growth-suppression activity. *Nat. Genet.* **2001**, *28*, 29–35.
12. Yu, L.; Liu, C.; Vandeusen, J.; Becknell, B.; Dai, Z.; Wu, Y.Z.; Raval, A.; Liu, T.H.; Ding, W.; Mao, C.; *et al.* Global assessment of promoter methylation in a mouse model of cancer identifies ID4 as a putative tumor-suppressor gene in human leukemia. *Nat. Genet.* **2005**, *37*, 265–274.
13. Hatada, I. *An Omics Perspective on Cancer Research*; Cho, W.C.S., Ed.; Springer: Dordrecht, The Netherlands, 2010; pp. 51–68.
14. Brenet, F.; Moh, M.; Funk, P.; Feierstein, E.; Viale, A.J.; Socci, N.D.; Scandura, J.M. DNA methylation of the first exon is tightly linked to transcriptional silencing. *PLoS One* **2011**, *6*, doi:10.1371/journal.pone.0014524.
15. Ohki, I.; Shimotake, N.; Fujita, N.; Jee, J.; Ikegami, T.; Nakao, M.; Shirakawa, M. Solution structure of the methyl-CpG binding domain of human MBD1 in complex with methylated DNA. *Cell* **2001**, *105*, 487–497.
16. Fairchild, C.R.; Ivy, S.P.; Kao-Shan, C.S.; Whang-Peng, J.; Rosen, N.; Israel, M.A.; Melera, P.W.; Cowan, K.H.; Goldsmith, M.E. Isolation of amplified and overexpressed DNA sequences from adriamycin-resistant human breast cancer cells. *Cancer Res.* **1987**, *47*, 5141–5148.
17. David, G.L.; Yegnasubramanian, S.; Kumar, A.; Marchi, V.L.; de Marzo, A.M.; Lin, X.; Nelson, W.G. MDR1 promoter hypermethylation in MCF-7 human breast cancer cells: Changes in chromatin structure induced by treatment with 5-Aza-cytidine. *Cancer Biol. Ther.* **2004**, *3*, 540–548.
18. Graff, J.R.; Herman, J.G.; Lapidus, R.G.; Chopra, H.; Xu, R.; Jarrard, D.F.; Isaacs, W.B.; Pitha, P.M.; Davidson, N.E.; Baylin, S.B. E-cadherin expression is silenced by DNA hypermethylation in human breast and prostate carcinomas. *Cancer Res.* **1995**, *55*, 5195–5199.
19 Ai, L.; Kim, W.J.; Demircan, B.; Dyer, L.M.; Bray, K.J.; Skehan, R.R.; Massoll, N.A.; Brown, K.D. The transglutaminase 2 gene (TGM2), a potential molecular marker for chemotherapeutic drug sensitivity, is epigenetically silenced in breast cancer. *Carcinogenesis* **2008**, *29*, 510–518.
20. Ozsolak, F.; Poling, L.L.; Wang, Z.; Liu, H.; Liu, X.S.; Roeder, R.G.; Zhang, X.; Song, J.S.; Fisher, D.E. Chromatin structure analyses identify miRNA promoters. *Genes. Dev.* **2008**, *22*, 3172–3183.

21. Shimono, Y.; Zabala, M.; Cho, R.W.; Lobo, N.; Dalerba, P.; Qian, D.; Diehn, M.; Liu, H.; Panula, S.P.; Chiao, E.; *et al.* Downregulation of miRNA-200c links breast cancer stem cells with normal stem cells. *Cell* **2009**, *138*, 592–603.
22. Gregory, P.A.; Bert, A.G.; Paterson, E.L.; Barry, S.C.; Tsykin, A.; Farshid, G.; Vadas, M.A.; Khew-Goodall, Y.; Goodall, G.J. The miR-200 family and miR-205 regulate epithelial to mesenchymal transition by targeting ZEB1 and SIP1. *Nat. Cell Biol.* **2008**, *10*, 593–601.
23. Tryndyak, V.P.; Beland, F.A.; Pogribny, I.P. E-cadherin transcriptional down-regulation by epigenetic and microRNA-200 family alterations is related to mesenchymal and drug-resistant phenotypes in human breast cancer cells. *Int. J. Cancer* **2010**, *126*, 2575–2783.
24. Hellman, A.; Chess, A. Gene body-specific methylation on the active X chromosome. *Science* **2007**, *315*, 1141–1143.
25. Wu, H.; Coskun, V.; Tao, J.; Xie, W.; Ge, W.; Yoshikawa, K.; Li, E.; Zhang, Y.; Sun, Y.E. Dnmt3a-dependent nonpromoter DNA methylation facilitates transcription of neurogenic genes. *Science* **2010**, *329*, 444–448.
26. Selvakumar, T.; Gjidoda, A.; Hovde, S.L.; Henry, R.W. Regulation of human RNA polymerase III transcription by DNMT1 and DNMT3a DNA methyltransferases. *J. Biol. Chem.* **2012**, *287*, 7039–7050.
27. Marshall, L.; White, R.J. Non-coding RNA production by RNA polymerase III is implicated in cancer. *Nat. Rev. Cancer* **2008**, *8*, 911–914.
28. Bird, A.P. CpG-rich islands and the function of DNA methylation. *Nature* **1986**, *321*, 209–213.

OPEN ACCESS Freely available online

PLOS | ONE

Comprehensive miRNA Expression Analysis in Peripheral Blood Can Diagnose Liver Disease

Yoshiki Murakami[1]*, Hidenori Toyoda[2], Toshihito Tanahashi[3], Junko Tanaka[4], Takashi Kumada[2], Yusuke Yoshioka[5], Nobuyoshi Kosaka[5], Takahiro Ochiya[5], Y-h Taguchi[6]

1 Department of Hepatology, Graduate School of Medicine, Osaka City University, Osaka, Japan, **2** Department of Gastroenterology, Ogaki Municipal Hospital, Ogaki, Japan, **3** Department of Medical Pharmaceutics, Kobe Pharmaceutical University, Kobe, Japan, **4** Department of Epidemiology, Infectious Disease Control and Prevention, Hiroshima University Graduate School of Biomedical Sciences, Hiroshima, Japan, **5** Division of Molecular and Cellular Medicine, National Cancer Center Research Institute, Tokyo, Japan, **6** Department of Physics, Chuo University, Tokyo, Japan

Abstract

Background: miRNAs circulating in the blood in a cell-free form have been acknowledged for their potential as readily accessible disease markers. Presently, histological examination is the golden standard for diagnosing and grading liver disease, therefore non-invasive options are desirable. Here, we investigated if miRNA expression profile in exosome rich fractionated serum could be useful for determining the disease parameters in patients with chronic hepatitis C (CHC).

Methodology: Exosome rich fractionated RNA was extracted from the serum of 64 CHC and 24 controls with normal liver (NL). Extracted RNA was subjected to miRNA profiling by microarray and real-time qPCR analysis. The miRNA expression profiles from 4 chronic hepatitis B (CHB) and 12 non alcoholic steatohepatitis (NASH) patients were also established. The resulting miRNA expression was compared to the stage or grade of CHC determined by blood examination and histological inspection.

Principal Findings: miRNAs implicated in chronic liver disease and inflammation showed expression profiles that differed from those in NL and varied among the types and grades of liver diseases. Using the expression patterns of nine miRNAs, we classified CHC and NL with 96.59% accuracy. Additionally, we could link miRNA expression pattern with liver fibrosis stage and grade of liver inflammation in CHC. In particular, the miRNA expression pattern for early fibrotic stage differed greatly from that observed in high inflammation grades.

Conclusions: We demonstrated that miRNA expression pattern in exosome rich fractionated serum shows a high potential as a biomarker for diagnosing the grade and stage of liver diseases.

Citation: Murakami Y, Toyoda H, Tanahashi T, Tanaka J, Kumada T, et al. (2012) Comprehensive miRNA Expression Analysis in Peripheral Blood Can Diagnose Liver Disease. PLoS ONE 7(10): e48366. doi:10.1371/journal.pone.0048366

Editor: Xiao-Ping Miao, MOE Key Laboratory of Environment and Health, School of Public Health, Tongji Medical College, Huazhong University of Science and Technology, China

Received May 17, 2012; **Accepted** September 24, 2012; **Published** October 31, 2012

Funding: Y.M, J.T, and T.K. were financially supported by the Ministry of Health, Labour and Welfare of Japan (H22-general-008)and Y.M, J.T, T.K, and Y.T received Grants-in-Aid for scientific research from the Ministry of Education, Culture, Sports, Science and Technology (22590727). The funders had no role in study design, data collection and analysis, decision to publish, or preparation of the manuscript.

Competing Interests: The authors have declared that no competing interests exist.

* E-mail: m2079633@med.osaka-cu.ac.jp

Introduction

MicroRNAs (miRNAs) are a gene family that is evolutionarily conserved and have important roles in the control of many biological processes, such as cellular development, differentiation, proliferation, apoptosis, and metabolism [1]. Aberrant expression of miRNAs in liver tissue has been implicated in the progression of liver fibrosis, and hepatocarcinogenesis [2,3,4]. Recently, two independent groups showed that miR-122 plays a critical role in the maintenance of liver homeostasis and anti-tumor formation [5,6].

Exosome in one of the endoplasmic reticulum carries mRNAs and miRNAs [7]. Recently, it has become clear that exosome perform intercellular signaling through miRNA. miRNAs are released through a ceramide-dependent secretory machinery and are then transferred and become functional in the recipient cells [8]. In a prior study using human blood and cultured cells, several miRNAs were selectively packaged into microvesicle (MV) and actively secreted [9]. In another study, miRNAs originating from EBV was transported by exosome and then participated in the immune response of host cells [10]. In HCC cells as well, this type of exosome-mediated miRNA transfer is an important mechanism of intercellular communication [11].

It has also become clear that exosome can adjust to immune function, control infection or carry the virus itself. Exosomes of T, B and dendritic immune cells contain a repertoire of miRNAs that differ from that of their parent cells [12,13]. Exosomes released from nasopharyngeal carcinoma cells harboring latent EBV were shown to contain LMP1, signal transduction molecules, and virus-encoded miRNAs [14]. Retroviruses evade adaptive immune responses by using nonviral or host exosome biogenesis pathways to form infectious particles and as a mode of infection [15].

Recent evidence has shown that the expression patterns of serum or plasma miRNAs are altered in several diseases, in particular heart disease, sepsis, malignancies, and autoimmune diseases (reviewed in [16]). Discoveries such as this is encouraging and has propelled further research leading to the hypothesis that circulating miRNAs are detectable in serum and plasma in a form sufficiently stable to serve as biomarkers [17,18]. One such example is that tumour-associated miRNAs were found in the serum of diffuse large B-cell lymphoma patients [19]. In other examples, serum levels of miR-34a and miR-122 were associated with histological disease severity in patients with CHC or non-alcoholic fatty-liver disease (NAFLD) [20]. In fact, the serum level of miR-122 strongly correlates with serum ALT activity and with necro-inflammatory activity in patients with CHC and elevated ALT levels. However, there seems to be no significant correlation between fibrosis stage and functional capacity of the liver [21]. The expression levels of miR-122 and miR-194 correlated negatively with age in patients with CHB and HBV associated acute-on-chronic liver failure [22]. The expression level of miR-122 in serum was found to be closely related to non drug-induced acute liver injury [23]. Based on the above, it comes as no surprise that recently, the expression profile from extracellular miRNA is being used clinically to diagnose various diseases.

Here, in order to obtain data with high resolution that is reproducible, we extracted MVs from serum using exoquick and then performed a comprehensive microarray analysis. We attempted to diagnose HCV infection, and ascertain the degree of liver inflammation and fibrosis stage using exosome-rich fractioned miRNA. In short, we investigate if serum-derived miRNAs had the potential to serve as non-invasive bio-markers for various liver diseases.

Results

Reproducible Gene-analysis Using Microarray

In microarray experiments, serum analysis is comparatively easy; however, the downside is that the accuracy and reproducibility of the results are usually not satisfactory. To circumvent this drawback, we devised a procedure that would give us higher accuracy and reproducibility. Serum samples from NL subjects were prepared and divided into two groups; for the first, RNA was extracted using exoquick treated serum, and in the second, RNA was extracted from total serum. Next, miRNA expression was analyzed using Agilent miRNA microarray. The above procedure was performed independently twice (**Fig. 1A**). We compared the miRNA expression pattern among the four microarray results (**Fig. 1B**) and found that miRNA expression analysis using exoquick was the more reliable and reproducible (**Fig. 1C**).

Exosome from normal human prostatic cell lines PNT-2, was yielded by the conventional ultra-centrifugation method [8]. We prepared serums with and without exoquick treatment and performed immunoblot analysis with anti-CD63 (**Fig. 1D**). Bands of the expected relative sizes were detected in serum treated with exoquick. We designated RNA extracted using exoquick treated serum as exosome-rich fractionated RNA.

Unique Expression Pattern of miRNA in CHC

We attempted to diagnose CHC using the miRNA expression pattern found in the peripheral blood samples from 64 CHC and 24 NL. The expression of nine miRNAs (miR-1225-5p, miR-1275, miR-638, miR-762, miR-320c, miR-451, miR-1974, miR-1207-5p, and miR-1246) allowed us to categorize patients as CHC or NL with 96.59% accuracy (**Fig. 2, 3** Table 1 and Table S1). As shown in **Fig. 2C**, CHC and NL were well differentiated due to their distinct miRNA expression patterns. The expression pattern of 12 miRNAs led to the distinction of CHC, CHB, NASH, and NL with 87.50% accuracy (**Fig. 4, S1A,** and Table S1). The accuracy of determining whether samples were CHC or CHB, CHC or NASH, CHB or NASH was 98.35%, 97.37%, and 87.50%, respectively. The accuracy of judging whether samples were NL or CHB, NL or NASH, was 89.29% and 88.89%, respectively (**Fig. 3, S1B** and Table S1). Unlike CHC and NL, there were relatively fewer analyses done of CHB and NASH (due to a small sample size), therefore, we used *"in silico"* resampling to overcome any possible bias. With *"in silico"* we found that it was highly reproducible to determine with high accuracy whether samples were CHC, CHB, NASH, or NL, CHC or CHB, CHC or NASH, CHC or NL, CHB or NASH, CHB or NL, or finally NASH or NL (**Fig. S2 to S8** and Supporting Information).

In order to validate our above-mentioned classifications, we prepared a separate independent sample consisting of 31 CHC, 16 CHB, and 8 NASH. We established miRNA expression patterns using microarray for each of these chronic liver disease groups. We tried to discriminate among the classifications in the independent cohort using the semi-supervised learning method [24] based only on the labels in the original sample group and the selected miRNAs shown in Table S1. The accuracy of judging whether samples were CHB or CHC, CHC or NASH, CHB or NASH, was 74.47%, 87.18%, and 79.19%, respectively (**Fig. S9**, Table 1, and Supporting Information). During the process of obtaining these results, we noticed that different versions of the Feature Extraction (FE) Software provided slightly different results, however it was not possible to fully unify these versions of FE. This may explain the relatively lower performance of the independent group compared with the original samples that mostly used the same FE Software versions.

miRNA Expression Correlates with the Grade of Liver Inflammation

The grade of inflammation for CHC patients was ascertained by liver histological examination, and then samples were divided into four groups A0, A1, A2, and A3 based on their fibrosis stage. miRNA expression profiles were then established for CHC according to each of their inflammation grade. From the four groups (A0 to A3), a combination of six arbitrary pairs is possible. miRNAs which had significant differential expression in five or more of the six pairs were extracted ($p<0.05$). Five miRNAs (miR-1914*, miR-193a-5p, miR-22, miR-659, and miR-711) had expression levels that increased as the severity of liver inflammation progressed. On the other hand, the expression levels of nine miRNAs (miR-1274b, miR-197, miR-1974, miR-21, miR-34a, miR-451, miR-548d-5p, miR-760, and miR-767-3p) significantly decreased with the progression of liver inflammation (**Fig. 5, S10** and Table S2).

The Grade of Liver Fibrosis Corresponded with the Expression Level of miRNAs

As previously noted, CHC samples were divided into F0, F1, F2, and F3 based on patients' fibrotic stage. From these four fibrotic groups, a combination of six arbitrary pairs were possible. miRNAs that had significant differential expression in all six pairs were extracted ($p<0.05$). The expression levels of two miRNAs (miR-483-5p and miR-671-5p) significantly increased the higher the fibrotic stage and the expression level of 14 miRNAs (let-7a, miR-106b, miR-1274a, miR-130b, miR-140-3p, miR-151-3p, miR-181a, miR-19b, miR-21, miR-24, miR-375, miR-548l, miR-93, and miR-941) became progres-

A

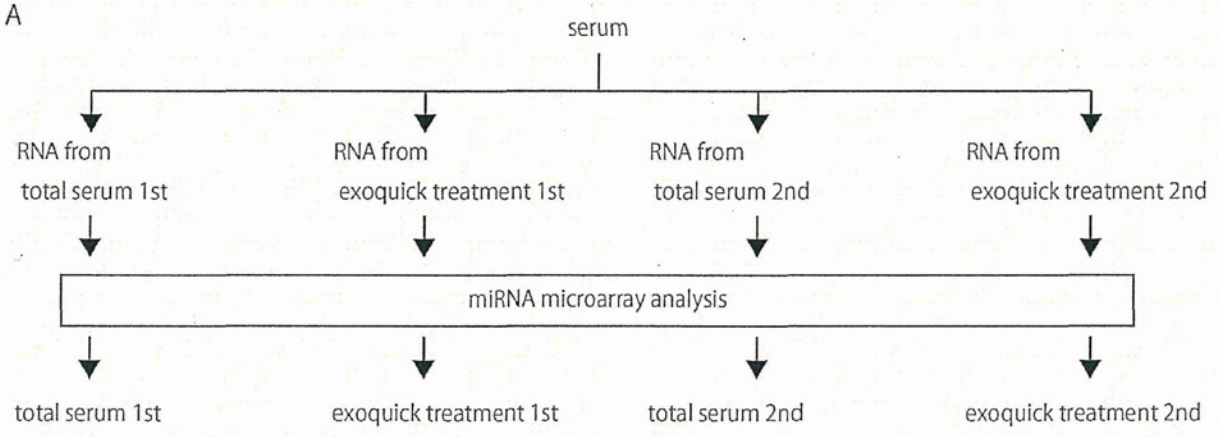

B

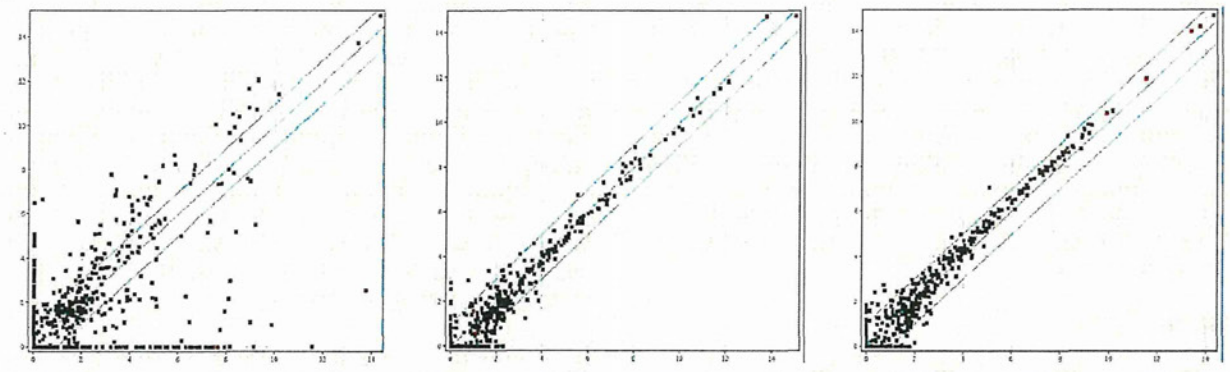

C

	exoquick 1st	total serum 1st	exoquick 2nd	total serum 2nd
exoquick 1st	1	0.836	0.998	0.809
total serum 1st	–	1	0.831	0.930
exoquick 2nd	–	–	1	0.821
total serum 2nd	–	–	–	1

D

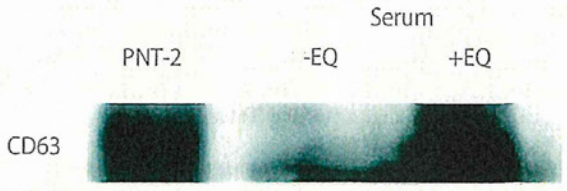

Figure 1. The method used to obtain reproducible data for microarray analysis conducted on serum-extracted samples. A. NL patients' serum were sampled twice. In the first, RNA was extracted first from untreated serum, and then extracted again from serum treated with exoquick. In the second serum sample, RNA was also extracted from both untreated serum and serum treated with exoquick. Microarray analysis was conducted for RNA in a total of four samples. B. Reproducibility test of microarray data. Scatter plots comparing non- normalized signal intensities of miRNAs in two independent experiments from human total serum and exosome rich fraction. Red and black denotes high and low miRNA expressions respectively. Total serum extracted first, versus exosome rich fraction first (left), total serum extracted first versus second (middle), and exosome rich fraction extracted first versus second (right). C. Pearson's pairwise correlations of signal intensities of miRNAs from human total serum and exosome rich fraction. D. Western blot was performed for untreated serum, serum extracted by exoquick and exosome fraction from PNT-2, using anti-CD63.

doi:10.1371/journal.pone.0048366.g001

A

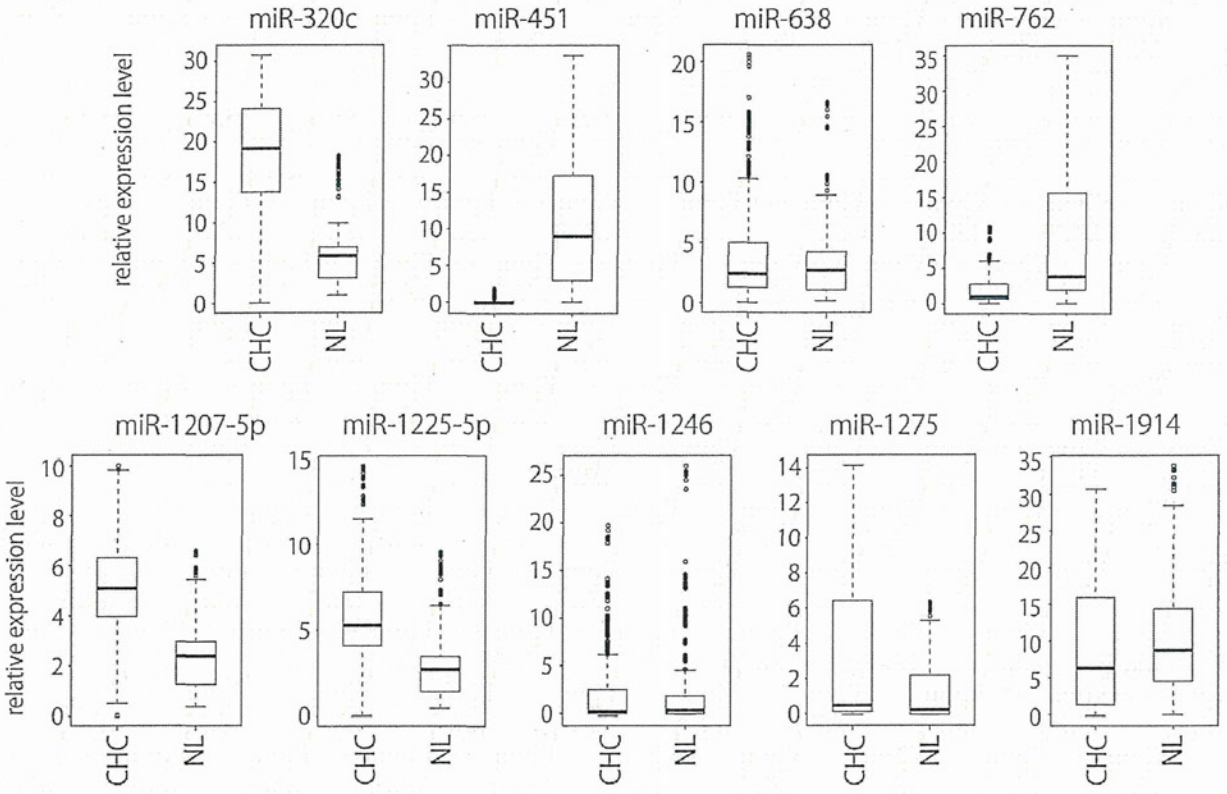

B

		result	
		CHC	NL
prediction	CHC	64	3
	NL	0	21

accuracy 96.6%

C

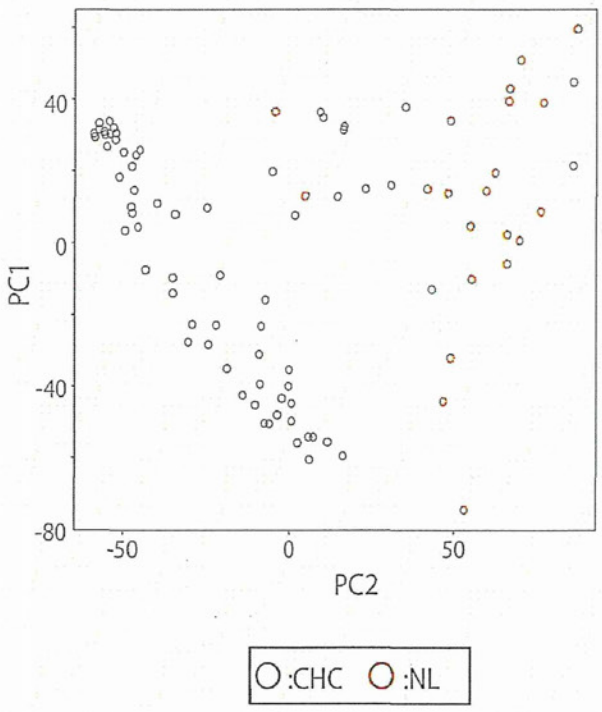

Figure 2. Expression patterns of miRNA used for discriminating between CHC and NL. A. Box plots of expression patterns of the nine miRNAs used for discriminating between CHC and NL. B. Classification of CHC and NL using LOOCV from miRNA expression profile. C. PCA in CHC and NL. The two dimensional embedding of CHC and NL by PCA. The first and second principal component scores computed (not selected for discrimination) of normalized miRNA expression were employed for this plot. Computation was done with ALL.
doi:10.1371/journal.pone.0048366.g002

sively downregulated as liver fibrotic stage increased (**Fig. 6, S11** and Table S2).

Classification of Liver Inflammation Grade and Fibrotic Stage Using miRNA Expression Pattern

We attempted to classify liver inflammation grade and fibrosis stage using miRNA expression pattern. Liver inflammation was diagnosed by Leave One Out Cross-Validation (LOOCV); the accuracy of determining A1 from other inflammation grade was 71.88% and its odds ratio was 7.08. The accuracy of determining A2 and A3 was 75.00% and 82.81%, and their odds ratios were 9.50 and 11.08, respectively. In our study, we were unable to accurately classify A0 because we were limited to only one sample for that grade (**Fig. 7A**). Diagnosis of liver fibrosis by LOOCV showed that determining F0 from the other fibrotic stages had an accuracy of 87.50% and an odds ratio of 14.25. The classification of F1, F2, and F3 had accuracy rates of 65.63%, 70.31%, and 73.44% and odds ratio of 3.16, 6.39 and 5.80, respectively (**Fig. 7B**).

miRNA Expression Level Detected by Real-time qPCR Validated the Microarray Result

Four miRNAs (miR-1207-5p, miR-134, miR-1249, and miR-1183) with expression levels that differed among liver inflammation grades and liver fibrotic stages were chosen in order to confirm the microarray results using stem-loop based real-time qPCR. miRNAs that correlated with other clinical characteristics besides liver fibrosis and inflammation were listed using the Wilcoxon test. We performed two Wilcoxon tests and ranked miRNAs based on their p-value from smallest to largest and selected the miRNAs with the four smallest p-values that were common among the two Wilcoxon tests.

The real-time qPCR result was consistent with the microarray analysis (**Fig. 8**). Here also, we applied *"in silico"* resampling to compensate for the small number of patients used in the real-time qPCR analysis. The results of the *"in silico"* resampling conferred with the results of the real-time qPCR (**Fig. S12**).

miRNA Expression Pattern was Closely Related to Several Clinical Parameters in CHC

Although we observed that miRNA expression correlated with ALT value, we were unable to identify miRNAs that displayed a strong correlation. 12 miRNAs were chosen sequentially from miRNAs with a high absolute correlation coefficient. One to 12 of these selected miRNAs were used to compare the canonical correlation coefficient of the above. When the expression patterns of six of the 12 miRNAs were compared with serum ALT value, the correlation coefficient and p-value were 0.44 and 4.91E−02, respectively. Similarly, when serum Albumin value was compared with the expression pattern of all 12 miRNAs, the correlation coefficient and p-value were 0.59 and 2.04E−02, respectively. Finally when the amount of serum HCVRNA was compared with the expression pattern of 12 miRNAs, the resulting correlation coefficient and p-value were 0.59 and 1.89E−02, respectively (**Fig. 9, S13** and Table S3).

Expression Pattern of a Several miRNAs Correlated to Serum and Hepatic Tissue

In a previous report, we described the miRNA expression pattern found in liver tissues obtained from 105 CHC [2]. From this group, we analyzed the miRNA expression of hepatic tissue and serum in 60 samples. We observed that the expression pattern of three miRNAs (miR-134, miR-200b, miR-324-5p) in hepatic tissue negatively correlated with that in serum, and the expression pattern of miR-370 in hepatic tissue positively correlated with that in serum ($p<0.05$) (Table S4). However, there was no significant correlation between the expression pattern of miR-122 in the hepatic tissue and serum (**Fig. S14** and Table S4).

Discussion

In this comprehensive miRNA analysis in various chronic liver diseases, we observed that aberrant expression of miRNAs was closely related to disease progression. Based on this, we believe that these miRNAs are potential readily accessible biomarkers, useful for diagnosing hepatic viral infection and for grading or staging liver diseases.

Many investigators have elected to use miRNA from serum instead of miRNA from exosome as the candidate for diagnosing diseases [18,20,22,25,26]. In our study, when exoquick was used, exosome could not be isolated therefore other MVs similar in size to exosome were also extracted. In other words, exoquick not only collected miRNAs contained in exosome, but also miRNA that were or were not combined with protein. Despite this, we found that exoquick delivered results that were superior to those obtained without exoquick. Therefore, although the process of analyzing miRNA from serum is simple, we chose to analyze miRNA from exosome rich fraction since it has a higher rate of reproducibility. Moreover, since exosome is closely related to intercellular signaling [14,27], it is expected that data obtained by exosome analysis can clarify the mechanism of chronic infection and inflammation [28].

When we extended our analysis from miR-122 to all miRNAs, it became clear that the expression level of several miRNAs correlated with the progression of liver fibrosis. In fact, recent studies have stated that when the expression levels of adequate numbers of miRNAs is used to identify disease, diagnostic ability is significantly higher than using a single miRNA [29]. In this study, when liver fibrosis was diagnosed using miRNA expression, distinguishing between F0 and F1-3 was done with 87.50% accuracy. Since F0 cannot be distinguished from other stages of chronic liver disease using blood examination, we propose that using miRNA expression pattern may be useful for diagnosing chronic liver disease that is in the early stage.

Previous studies have shown that the level of miR-122 in blood plasma increased earlier than in ALT in the presence of toxic liver injury in rodents [30]. Serum levels of miR-122 in patients with CHC are frequently elevated compared with healthy individuals [21]. Bihrer et al. mentioned that variations in the concentration of miR-122 in serum or plasma tend to be more specific for liver diseases than ALT and AST. This is because miR-122 is almost exclusively expressed in the liver, whereas ALT and AST originate from skeletal muscles and other tissues, therefore their diagnostic value is low [31]. In our study, the expression level of miR-122 had